

An analytical approach towards EHD analysis of connecting-rod bearing

A. Benhamou*, **A. Bounif****, **P. Maspeyrot*****, **C. Mansour******

*Faculty of Technology, Hassiba Benbouali University, B.O. 151, Chlef, 02000, Algeria, E-mail: abdbenhamou@yahoo.fr

**LCGE Laboratory, USTO Mohamed Boudiaf University, BO 1505, Oran, 31000, Algeria, E-mail: abounif@yahoo.com

***Pprime Institute, Structure and Complex Systems Department, B.O. 30179, Poitiers 86000, France

E-mail: patrick.maspeyrot@univ-poitiers.fr

****LCGE Laboratory, USTO Mohamed Boudiaf University, BO 1505, Oran, 31000, Algeria,

E-mail: abdelbounif@yahoo.com

 <http://dx.doi.org/10.5755/j01.mech.20.2.6935>

Nomenclature

A_x - dynamic factor of amplification for the longitudinal deformation; A_θ - dynamic factor of amplification for the radial deformation; $[C]$ - matrix of rigidity; $[D]$ - matrix of the compression forces; E - Young modulus; h - oil film thickness; $H(x)$ - heaviside distribution; $P(x,t)$ - hydrodynamic pressure; R - average radius of the bearing; t - time; $U(x,t)$ - longitudinal displacement; V - linear speed; V_b - speed propagation of the longitudinal wave; V_p - speed propagation of the radial wave; $W(x,t)$ - radial displacement; x - axial coordinate; $[\varepsilon]$ - deformation vector; ε_x - longitudinal deformation; ε_θ - radial deformation; ν - Poisson's ratio; ω - rod-bearing frequency; ρ - density; σ_x - longitudinal constraint; σ_θ - transversal constraint; θ - angular position.

1. Introduction

Tribology field aims to understand interaction problems between surfaces while suggesting specific solutions. It concerns lubrication, wear as well as contact mechanics. The expanding range of tribological applications, from early machinery applications to recently micro and nano applications, has not only demonstrated its importance but revived recent interests of the field. The introduction of a range of micro-fabrication techniques coupled with developments in materials design has had a profound effect on the resurgence of tribological applications at the friction levels [1]. Competition in the automotive industry as well as the requirements of customers requires manufacturers to reduce pollution and consumption while improving engine performance [2]. In this context many experimental and numerical studies were developed within this research area. Among the studies, one can distinguishes the elastohydrodynamic (EHD) lubrication domain for smooth bearings for which the lubricant film interacts with solid surfaces, yielding specific behaviours, as it is the case for connecting-rod bearings in IC engines. Steady state behaviour of journal bearing has recently been investigated numerically by Kumar et al [3]. Despite six decades of EHD lubrication studies, safety and reliability improvement of journal bearing under dynamic loading is still considered as a challenging task. The kinematics and dynamics of the operation of such journal bearings generate a field of pres-

sure inside the oil film which in turn creates a deformation on the surfaces of the bearing and the journal. On the other hand, solid deformations generate local modifications in the lubricant thickness while affecting the pressure distribution within the oil film. In the early works of Fantino et al [4], some numerical solutions of the EHD problems were obtained using a fourth order Runge-Kutta integration. Simultaneously, journal bearing under dynamic loading were concerned with the finite element Oh and Goenka [5]. Fantino et al [6] have shown that the elastic strain of the structures and the location at which the thickness is minimal are nearly independent of the viscosity of the lubricant and that the friction and the axial flow are more important in the elastic case than in the rigid case. To overcome numerical difficulties regarding finite element convergence, McIvor et al [7] advocate the necessity of using high order elements despite their important computational cost. The inertia influence of solids on the oil film thickness was evidenced by Aitken et al [8], and numerically confirmed in the work of Bonneau et al [9]. In this context, the authors have developed an EHD algorithm accounting for cavitation within journal bearings. In 1997, Garnier [10] approached the problem of EHD by considering the connection casing-crankshaft of a thermal engine. In 2000, Pif-feteau et al. [11] conducted a thermo-elastohydrodynamic study of a connecting-rod bearing in transitory mode. In the same content a recent work has been performed on heat transfer towards the oil film, and quantified using thermo-elastohydrodynamic (TEHD) [12]. In the work of Bonneau et al. [13], some modelling approaches were proposed for the prediction of break-off and formation of lubricant films within EHD contacts. The authors have stated out the necessity of accounting for inertia effects in the deformation prediction procedure. These statements were confirmed by Olson et al [14] when the authors investigated an elastic structure dynamics including inertia effect. The model has been applied to solve a coupled set of equations governing hydrodynamics with elasticity of a journal bearing [15]. In this work, an analytical resolution of the EHD problem is proposed for connecting-rod bearing engine. The procedure solves simultaneously the reduced form of the Reynolds equation as well as Hook equation. A space-time dependant variable is introduced in the set of equations in the aim to relate radial and longitudinal deformations. As an application case, a journal bearing of the General Motors

Diesel engine is investigated [16-17]. Inertia effects on the oil film thickness are evidenced under a moderate regime. Moreover, a parametric study regarding connecting-rod bearing material type is conducted towards an optimization insight.

2. Formulation

2.1. Hydrodynamic lubrication

Investigation of when the L/D ratio of the length to the diameter of the journal bearing is small, i.e. lower than $1/6$, the circumferential gradient of pressure can be neglected in front of the axial gradient of pressure [18]. Here one considers a connecting-rod bearing subjected to a dynamic head. The Reynolds equation in transitory mode is written as follows:

$$\frac{\partial}{\partial z} \left[\frac{\partial h^3}{\mu} \frac{\partial p}{\partial z} \right] = 12\rho(u_c - u_a) \frac{\partial h}{\partial x} + 6\rho h \frac{\partial}{\partial x} (u_c + u_a) + 12\rho v_a. \quad (1)$$

In the case of a smooth bearing, the external forces acting on the rod consist of the combustion pressure resultant within cylinders and inertia forces for the moving parts. The system is believed to be in equilibrium throughout the loading cycle. The balance can be written in vector-

$$\begin{cases} u_a = c\varepsilon^* \sin \varphi - c\varepsilon(\psi^* + \phi^*) \cos \varphi + R_a \omega_a \\ u_a = c\varepsilon^* \cos \varphi + c\varepsilon(\psi^* + \phi^*) \sin \varphi - c\varepsilon \omega_a \sin \varphi \end{cases} \quad \text{with} \quad \begin{cases} u_c = \omega_c R \\ v_c = 0 \end{cases}. \quad (3)$$

This yields a reduced form for the Reynolds equation:

$$\frac{\partial}{\partial \bar{z}} \left[\frac{\partial \bar{h}^3}{\mu} \frac{\partial \bar{p}}{\partial \bar{z}} \right] = \frac{12 \mu L D \rho (R/L)^2}{F(c/R)^2} \left[(\phi^* - \bar{\omega}) \varepsilon \sin \varphi + \varepsilon^* \cos \varphi \right], \quad (4)$$

where

$$h = \bar{h} c, \quad z = \bar{z} L, \quad p = \bar{p} F / (LD) \quad \text{and} \quad \bar{\omega} = \frac{\omega_a + \omega_c}{2} - \psi^*. \quad (5)$$

The speeds of crushing and rotation ε^* and ϕ^* are unknown factors in the problem. \bar{p} is the reduced pressure to be determined. In this work, an analytical approach is performed by means of the mobility method [19]. The so-called graphic method of calculating "mobility" makes it possible to calculate the trajectory of the journal in its housing. Two components for the journal movement are considered, the crushing and the rotation. These last define the mobility vector. This method is applied for the resolution of Eq. (3). In order to derive an analytical expression for the solution of Eq. (3), one makes a use of the mobility vector $\vec{M} (M_\varepsilon, M_\phi)$, so that:

$$\begin{cases} \varepsilon^* = \frac{F(c/R)^2}{\mu L D} M_\varepsilon \\ \varepsilon(\phi^* - \bar{\omega}) = \frac{F(c/R)^2}{\mu L D} M_\phi \end{cases} \quad (6)$$

rial form by accounting for external forces acting on the journal bearing and the force resulting from hydrodynamic pressure and inertia.

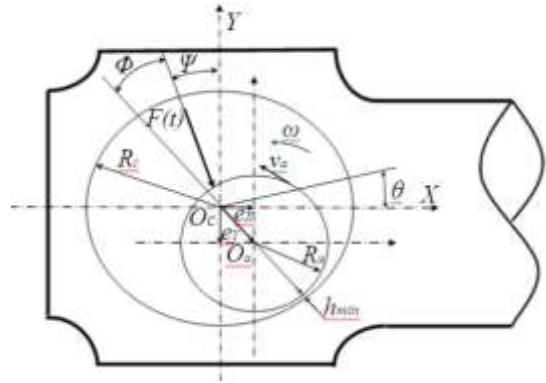


Fig. 1 Coordinates of the system

In the coordinate system (Fig. 1), the budget equations including the applied external force (load F) and the hydrodynamic reaction due to the pressure field, are as follows:

$$\begin{cases} F_\varepsilon = F \cos \phi = - \int p \cos \phi \, ds \\ F_\phi = F \sin \phi = - \int p \sin \phi \, ds \end{cases}. \quad (2)$$

Expressions for the various speeds of the journal u_a and of the bearing v_c , can be written as:

$M_\varepsilon = M \cos \alpha$ and $M_\phi = M \sin \alpha$ account for crushing and rotation effects, respectively. Some rearrangements on Eq (4) in (2) lead to a simplified form for the Reynolds equation:

$$\frac{\partial}{\partial \bar{z}} \left[\frac{\partial \bar{h}^3}{\mu} \frac{\partial \bar{p}}{\partial \bar{z}} \right] = 12(L/R)^2 M \cos(\theta + \alpha). \quad (7)$$

The appropriate boundary conditions are those of Gumbel [18]:

$$\bar{p}(\theta, \bar{z}) = \pm 1/2 \quad \text{and} \quad \bar{p}(\theta, \bar{z}) \geq 0. \quad (8)$$

The corresponding pressure distribution is therefore:

$$\bar{p}(\theta, \bar{z}) = 24 \frac{(L/D)^2}{h^3} \left(\frac{\bar{z}^2}{2} - \frac{1}{4} \right) M \cos(\theta + \alpha). \quad (9)$$

2.2. Elastic deformations

It is worthy noticing that both hydrodynamic pressure as well as inertia effects contributes to the elastic deformation of the connecting-rod bearing.

According to the works of Goenka et al. [16] and Bonneau et al. [17], the connecting-rod bearing deformation for each effect was calculated separately by means of a numerical procedure. In this work, one proposes an analytical approach for evaluating simultaneously this deformation. In a case where the bearing thickness is lower than the radius of the journal, the constraints within the bearing are assumed to be uniform. The journal operates at a constant speed while producing elastic deformations which are related to the longitudinal and radial constraints.

$$\begin{cases} \frac{h}{R} \sigma_\theta + \rho h \frac{\partial^2 w}{\partial t^2} = p(x, t) \\ \frac{\partial \sigma_x}{\partial x} = \rho \frac{\partial^2 u}{\partial t^2} \end{cases}, \quad (10)$$

$\varepsilon_x = \partial u / \partial x$ and $\varepsilon_\theta = w/R$ are the expressions of linear deformation, which are related to the plane constraints expressions by:

$$\begin{cases} \sigma_\theta = \frac{E}{1-\nu^2} \left(\frac{w}{R} + \nu \frac{\partial u}{\partial x} \right) \\ \sigma_x = \frac{E}{1-\nu^2} \left(\frac{\partial u}{\partial x} + \nu \frac{w}{R} \right) \end{cases}. \quad (11)$$

$$\begin{cases} \frac{\nu E}{1-\nu^2} \varepsilon_x + \frac{E}{1-\nu^2} \varepsilon_\theta + \rho R^2 V^2 \frac{d^2 \varepsilon_\theta}{dx^2} = \frac{R}{h} p(x) \\ \left(\frac{E}{1-\nu^2} - \rho V^2 \right) \varepsilon_x + \frac{\nu E}{1-\nu^2} \varepsilon_\theta = \left(\frac{E}{1-\nu^2} - \rho V^2 \right) \varepsilon_{x_0} + \frac{\nu E}{1-\nu^2} \varepsilon_{\theta_0} \end{cases}, \quad (14)$$

where $\varepsilon_{x_0} = (du/dx)_0$ and $\varepsilon_{\theta_0} = w_0/R$ denote for the initial deformations. A compact form for the system can be expressed as:

$$\begin{bmatrix} \rho R^2 & 0 \\ 0 & 0 \end{bmatrix} \begin{bmatrix} \varepsilon_\theta'' \\ \varepsilon_x'' \end{bmatrix} + \begin{bmatrix} \frac{E}{1-\nu^2} & \frac{\nu E}{1-\nu^2} \\ \frac{\nu E}{1-\nu^2} & \frac{E}{1-\nu^2} - \rho V^2 \end{bmatrix} \begin{bmatrix} \varepsilon_\theta \\ \varepsilon_x \end{bmatrix} = \begin{bmatrix} \frac{R}{h} p(\tau) \\ K \end{bmatrix}, \quad (15)$$

where K refers to the non-homogeneous part in the second equations of the set (13) and $\tau = \frac{X}{V}$ is a delay time. In a case where only progressive perturbations are considered, the pressure can be expressed as a step function:

$$p(\tau) = P.H \left(t - \frac{x}{V} \right) \quad \text{with } H = 1 \quad \text{when } x < V.t \quad (16)$$

and $H = 0$ when $x > V.t$,

where H denotes for the Heaviside distribution.

The obtained system can be simply written as:

$$[A] \{\varepsilon''\} + [C] \{\varepsilon\} = [D]. \quad (17)$$

The set of the partial differential Eq. (11) expresses the coupling between the bearing deformation and the hydrodynamic pressure. Under a mechanical equilibrium; the set becomes:

$$\begin{cases} \frac{E}{1-\nu^2} \frac{R}{h} \left(\frac{w}{R} + \nu \frac{\partial u}{\partial x} \right) + \rho R \frac{\partial^2 u}{\partial t^2} = \frac{R}{h} p(x, t) \\ \frac{E}{1-\nu^2} \left(\frac{\partial^2 u}{\partial x^2} + \frac{\nu}{R} \frac{\partial w}{\partial x} \right) = \rho \frac{\partial^2 u}{\partial t^2} \end{cases} \quad (12)$$

Far from the bearing axis, the origin of the deformation can be considered as a perturbation moving at a speed V . Consequently, the displacements U and W as well as the hydrodynamic pressures are related to dependent variable ($X = x - Vt$). Accordingly, the set (11) takes the following form:

$$\begin{cases} \frac{E}{1-\nu^2} \left(\frac{w}{R} + \nu \frac{du}{dx} \right) + \rho h V^2 \frac{d^2 w}{dx^2} = p(x) \\ \frac{E}{1-\nu^2} \left(\frac{d^2 u}{dx^2} + \frac{\nu}{R} \frac{dw}{dx} \right) = \rho V^2 \frac{d^2 u}{dx^2} \end{cases}. \quad (13)$$

Substituting du/dx and w/R by ε_x and ε_θ respectively; one obtains:

The general solution of system (15) is the sum of a particular solution $\{\varepsilon_0\}$ and a general solution of the associated homogeneous linear equation $\{\varepsilon_i\}$, in manner that:

$$\{\varepsilon\} = \{\varepsilon_0\} + \{\varepsilon_i\}. \quad (18)$$

The characteristic solution of Eq. (17) is as follows:

$$\varpi^2 = -\frac{E}{\rho R^2} \frac{E - \rho V^2}{E - \rho V^2 (1 - \nu^2)} = -\frac{V_p^2}{R^2} \frac{V^2 - V_b^2}{V^2 - V_p^2}, \quad (19)$$

with $V_b = (E/\rho)^{1/2}$ and $V_p = (E/\rho(1-\nu^2))^{1/2}$, V_b and V_p are respectively the propagation velocities of the longitudinal and radial elastic waves in the rod bearing.

The form of the solution $\{\varepsilon_i\}$ will depend on V , V_b and V_p as:

$$\begin{cases} \{\varepsilon_i\} = \{\varepsilon_{i1}\} e^{-\varpi\tau} + \{\varepsilon_{i2}\} e^{-\varpi\tau} & \text{for } V_b < V < V_p \\ \{\varepsilon_i\} = \{\varepsilon_{i1}\} \cos \varpi\tau + \{\varepsilon_{i2}\} \sin \varpi\tau & \text{for } V > V_p \text{ or } V < V_b \end{cases} \quad (20)$$

The second member of Eq. (17) becomes:

$$D = \begin{bmatrix} \frac{R}{h} P.H \left(t - \frac{x}{V} \right) \\ 0 \end{bmatrix}. \quad (21)$$

The expressions for the longitudinal and radial deformation are given by:

$$\begin{cases} \varepsilon_\theta = \frac{P R}{E h} (1 - \cos \varpi t) A_\theta \\ \varepsilon_x = \frac{\nu P R}{E h} (1 - \cos \varpi t) A_x \end{cases}, \quad (22)$$

where

$$\begin{aligned} A_\theta &= \frac{V_b^2 V^2 - V_p^2}{V_p^2 V^2 - V_b^2}, \quad A_x = \frac{V_b^2}{V_p^2} \frac{V_b^2}{V^2 - V_b^2} \quad \text{and} \\ \varpi &= \frac{V_p}{R} \left(\frac{V^2 - V_b^2}{V^2 - V_p^2} \right)^{1/2}. \end{aligned} \quad (23)$$

The two coefficients A_θ and A_x are related to the ratio V/V_p their expressions shows that:

- the radial deformation increases with an increase in V ;
- the longitudinal deformation increases as V decreases, with the evolution of A_x and pressure p ;
- the positive ratio $\varepsilon_x/\varepsilon_\theta = \nu V_p^2 / (V^2 - V_p^2)$, does not depend on pressure P and decreases as V increases.

3. Resolution procedure

As the right term of Eq. (7) depends only on the mobility direction α , the resolution is believed to be simple. In this context, an interpolation procedure is performed for a given attitude angle ϕ (Fig. 1) for each time step within the cycle. More details regarding the tabulation method of the mobility direction can be found in [19]. Here, for a given load diagram, the hydrodynamic pressure is obtained by solving Reynolds equation which allows for the determination of both longitudinal and radial deformations.

4. Results and discussion

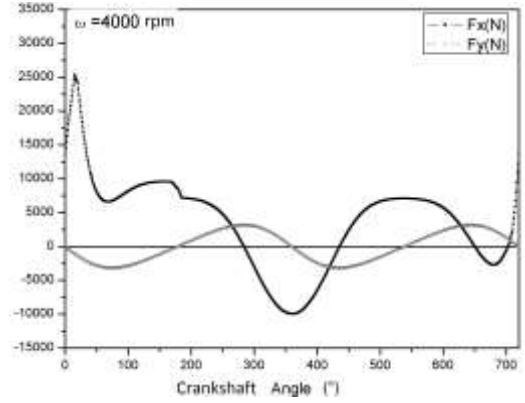
The journal bearing considered in this study is that of a Diesel General Motors engine, as investigated by Goenka et al [16] and Bonneau et al. [17]. Table 1 summarises the journal bearing characteristics.

According the work of Goenka et al [16], two regimes corresponding to 2000 rpm and 4000 rpm were considered. The corresponding load diagrams are shown in (Fig. 2).

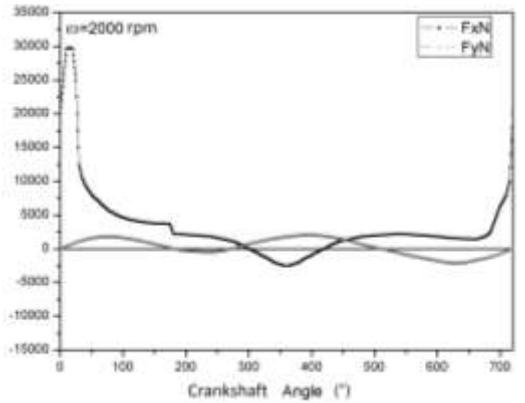
The loading was numerically fitted with a piece-

Characteristics of the connecting-rod bearing

Length of the journal bearing, mm	21.60
Length of the crank, mm	38.06
Length of the rod, mm	145
Diameter of the journal, mm	54
Ratio L/D	0.4
Radial clearance C , mm	0.027
Thickness of the bearing, mm	4
Young's modulus E , GPa	213.17
Poisson's ratio ν	0.30
Density of the material ρ , kg/m ³	7800
Lubricant viscosity μ , Pas	0.00689



a



b

Fig. 2 Forces diagram of the GM Diesel engine: a - 4000 rpm, b - 2000 rpm [16]

wise polynomial expression, and implemented within the calculation loop. For the particular speed of 4000 rpm, the calculations were performed for the specific case where the inertia effects are neglected. For a complete cycle of the engine operation, the minimum oil film thickness is compared to the results obtained by Goenka et al. [16] and Bonneau et al. [17] (Fig. 3).

One notices that the minimal film thickness for the three approaches, exhibits the same tendency. A slight deviation is noticed on the film thickness value which seems to be overestimated due to the short journal assumption, considered in the present work. In the following, the elastic strains are calculated with and without inertia effect by considering three types of material (Table 2). A parametric study regarding the materiel is also performed. Three types of materials are considered at both low (2000 rpm) and moderate (4000 rpm) regimes.

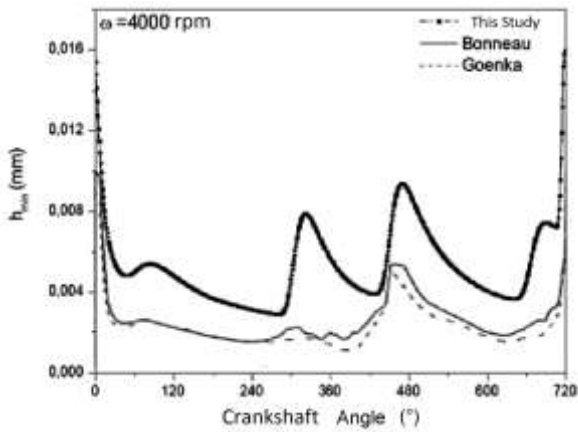
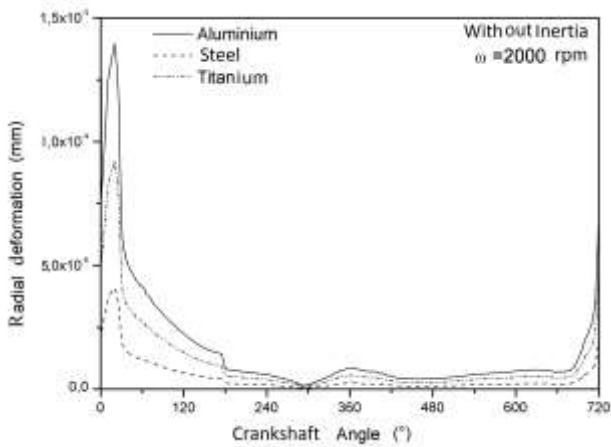


Fig. 3 Oil film thickness distribution without inertia effects

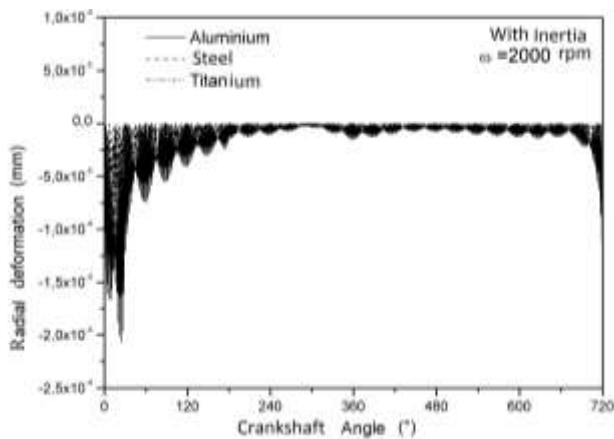
Table 2
Characteristics of the materials connecting-rod bearing materials

Material	Aluminium	Titanium	Steel
Young's modulus, GPa	69	114	213
Poisson's ratio	0.33	0.36	0.30
Density, kg/m ³	2700	4507	7800

Figure 4 shows, for the three materials, the evolution of the radial and longitudinal elastic strain with and without the effect of inertia induced by a dynamic loading corresponding to a speed of 2000 rpm.



a

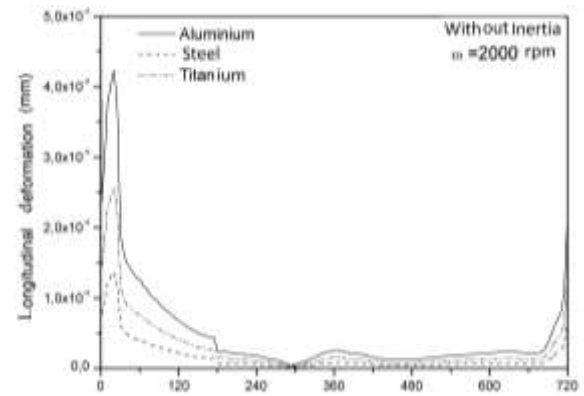


b

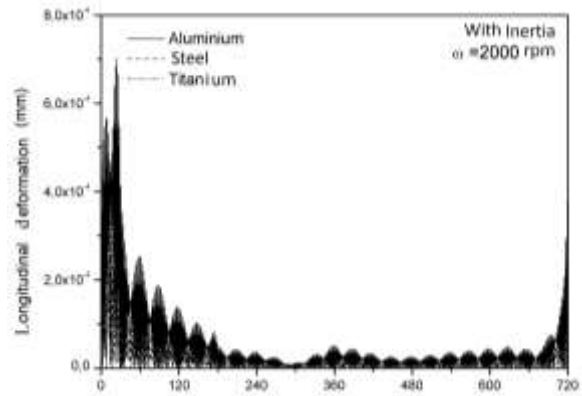
Fig. 4 Radial deformations: a - without inertia effect; b - with inertia effect

It is noticed that except for the oscillatory behaviour created by the non-stationary term of Eq. (21), the oscillations appearing in the material are described by the very significant frequencies. The deformations become negative, in contrast to their behaviour in the case where inertia effects were neglected. This specific behaviour due to the effects of inertia makes it possible to moderate the effects of dilation generated by the deformations induced by the governing hydrodynamic pressure appearing in the journal bearing.

One notices in Fig. 5, with regard to longitudinal deflection, that no modification is apparent except for the oscillations induced by the non-stationary term. Figure 6 shows the evolution of the minimal thickness of oil film with and without the effect of inertia for a cycle loading.



a



b

Fig. 5 Longitudinal deformations: a - without inertia effect; b - with inertia effect

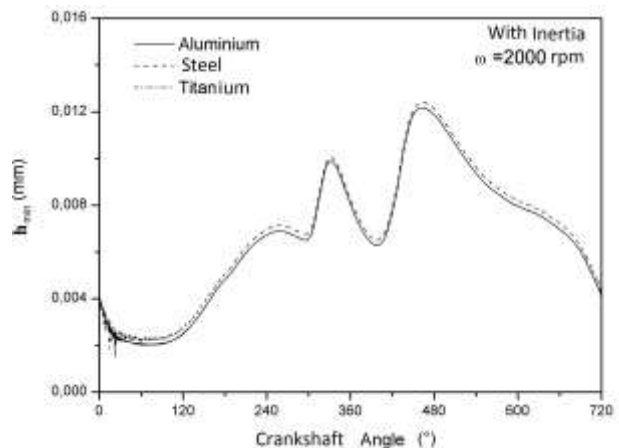
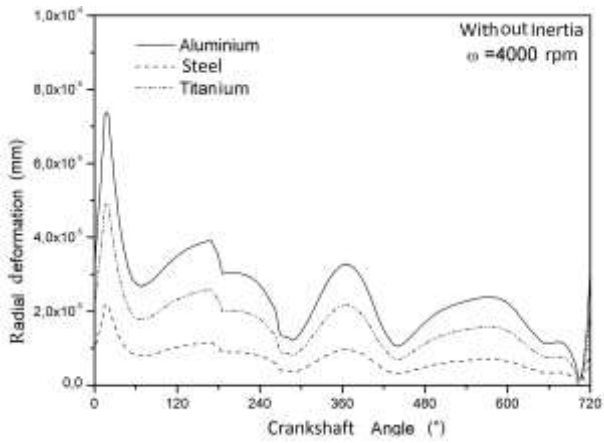
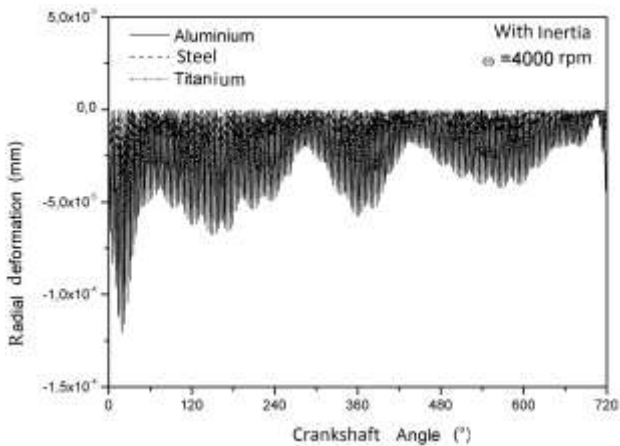


Fig. 6 Minimum oil film thickness for three materials

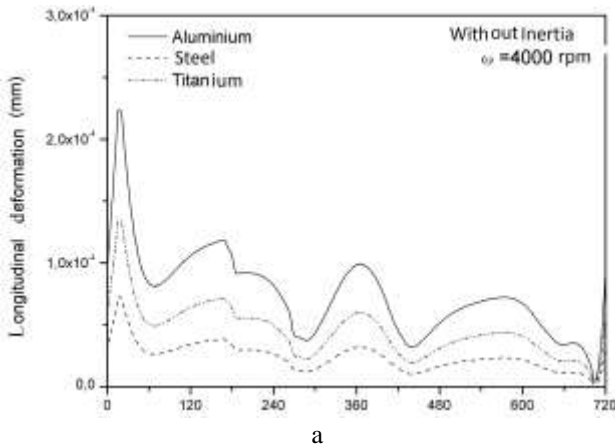


a

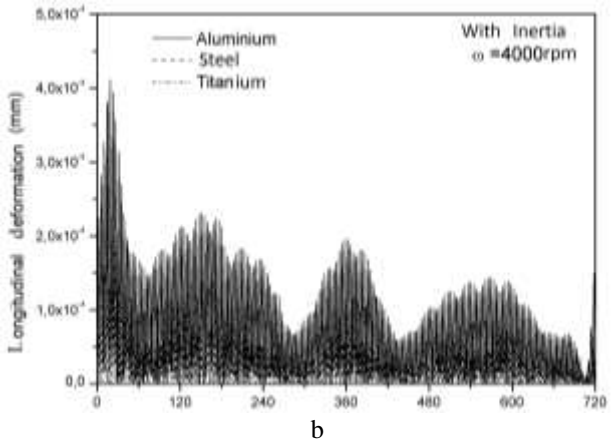


b

Fig. 7 Radial deformation: a - without inertia effect; b - with inertia effect



a



b

Fig. 8 Longitudinal deformation: a - without inertia effect; b - with inertia effect

The curve accounting for the effect of inertia, exhibits values lower than that without inertia effects. Consequently, the effects induced by inertia are relatively constraining on journal deformation at high-speeds.

In addition, in the case relating to the effects of inertia, the materials' influence becomes less consistent by the overall effect undergone by the deformation resulting from the superposition of the coupled influence of materials and the effects of inertia.

For the specific speed of 4000 rpm and for the three types of material considered the radial and longitudinal elastic strain with and without the effect of inertia are shown in (Figs. 7 and 8). The minimal thickness of the oil film calculated for $\omega = 4000$ rpm with and without the effect of inertia is shown in (Fig. 9). The same tendency is observed as for 2000 rpm. The effect of inertia and the material type on deformation have a more marked tendency, in particular for the radial deformations and their consequence on the minim oil film thickness.

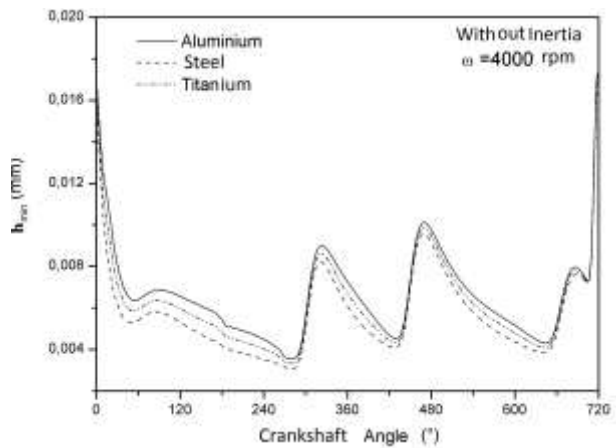


Fig. 9 Material effects on the minimum oil film thickness without inertia effect

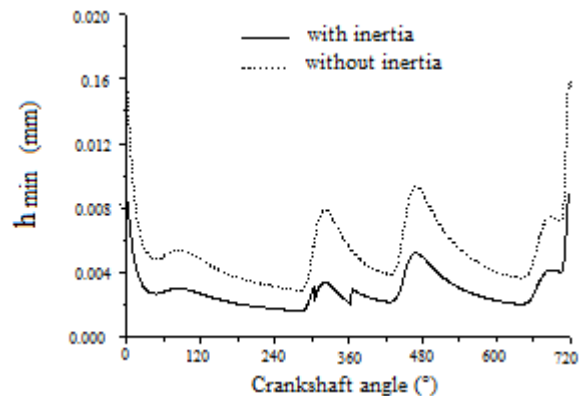


Fig. 10 Inertia effects on the minimum film thickness for the General Motors connecting-rod bearing at 4000 rpm

In Fig. 10, one clearly notices the correction introduced by the introduction of the effect of inertia, particularly, the clear difference between the results without the effects of inertia. The results obtained so far are very close to those obtained in the former work of Goenka et al. [16] and Bonneau et al. [17], despite the assumption of the short journal bearing introduced into the analytical calculation. The contact in the journal bearing, the elasto-hydrody-

dynamic machine part subjected to very harsh operating conditions, which is conducting the minimum reducing the density of the lubricant film which could be premature wear of the contact. In this situation, the load is applied on the rod journal bearing while yielding strong stresses. Despite the short journal assumption considered in the present case, the results appear to be fairly close to those of Goenka [16] and Bonneau [17].

5. Conclusion

Analytical approach was used in the purpose of predicting the deformations of a connecting-rod bearing subjected to inertia and hydrodynamic pressure effects. The results show that materials with low density exhibit important deformations while allowing for possible contacts, between surfaces. This behaviour seems to be significant at moderate (4000 rpm) and high regimes. Accounting for inertia effects, the results have confirmed the contribution of in the global deformation, particularly for the behaviour discrepancy with and without inertia effects. The curve accounting for inertia exhibits lower values than that without the inertia effects. Consequently, the effects induced by inertia are relatively constraining on journal deformation at high-speeds.

References

1. **Himashu C Patel; Deheri, G.M.** 2009. Characteristics of lubrication at nano scale on the performance of transversely rough slider bearing, *Mechanika* 6(80): 64-71.
2. **Moritsugu Kasai, Michel Fillon, Jean Bouyer and Sebastien Jarny.** 2012. Influence of lubricants on plain bearing performance: Evaluation of bearing performance with polymer-containing oils, *Tribology International* 46: 190-199.
<http://dx.doi.org/10.1016/j.triboint.2011.03.009>.
3. **Senthil Kumar, M.; Thyla, P.R.; Anbarasu, E.** 2010. Numerical analysis of hydrodynamic journal bearing under transient dynamic conditions, *Mechanika* 2(82): 37-42.
4. **Fantino, B.** 1981. Influence des Défauts de Forme et des Déformés Elastiques des Surfaces en Lubrification Hydrodynamique sous Charge Statiques et Dynamiques -Thèse de doctorat d'état n° 1-DE-8122, INSA de Lyon, France.
5. **Oh, K.P.; Goenka, P.K.** 1985. The elastohydrodynamic solution of journal bearings -under dynamic loading, *ASME journal of Tribology* 107: 389-395.
<http://dx.doi.org/10.1115/1.3261088>.
6. **Fantino, B.; Frêne, J.** 1985. Comparison of dynamic behaviour of elastic connecting-rod bearing in both petrol and diesel engines, *ASME Journal of Tribology* 107: 87-91.
<http://dx.doi.org/10.1115/1.3261007>.
7. **McIvor, J.D.C.; Fenner, D.N.** 1985. An evolution of eight-node quadrilateral finite elements for the analysis of a dynamically loaded hydrodynamic journal bearing, *Proc. Inst. Mech. Engrs.* 202: 95-101.
8. **Aitken, M.B.; McCallion, H.** 1991. Elastohydrodynamic lubrication of big-end bearings Part 1: Theory, *Proc. Instn. Mech. Engrs.* 205: 99-106.
http://dx.doi.org/10.1243/PIME_PROC_205_097_02.
9. **Bonneau, D.; Guines, D.; Frêne, J.; Toplosky, J.** 1995. EHD analysis, including structural inertia effects and a mass-conserving cavitation model, *ASME-Journal of Tribology* 117: 540-547.
<http://dx.doi.org/10.1115/1.2831288>.
10. **Garnier, T.** 1997. Etude Elastohydrodynamique de la Liaison Carter/Vilebrequin d'un Moteur Thermique à Quatre Cylindres en Ligne-PhD Thesis, UCL of University of Poitiers.
11. **Piffeteau, S.; Souchet, D.; Bonneau, D.** 1999. Influence of thermal and elastic deformations on connecting-rod big end bearing lubrication under dynamic loading-*ASME Journal of Tribology* 122: 181-191.
<http://dx.doi.org/10.1115/1.555341>.
12. **Mansouri, B.; Belarbi, A.; Imine, B.; Boualem, N.** 2013. Crankshaft journals bearings behavior under dilation and strain effects, *Mechanika* 19(5): 593-599.
<http://dx.doi.org/10.5755/j01.mech.19.5.5528>.
13. **Bonneau, D.; Hajjam, M.** 2001. Modélisation de la Rupture et de la Reformation des Films Lubrifiants dans les Contacts Elastohydrodynamiques, *European Review of Finite Elements* 10: 679-704.
<http://dx.doi.org/10.1080/12506559.2001.9737566>.
14. **Olson, E.G.; Booker, J.F.** 2001. EHD analysis with distributed structural inertia, *J. Tribol.* 123(3): 462-468.
<http://dx.doi.org/10.1115/1.1332396>.
15. **Fabrizio, A.; Stefani' Alessandro U. Reborra.** 2004. A nonlinear structure based elastohydrodynamic analysis method for connecting rod big end bearings of high performance engines, *J. Tribol.* 126(4): 664-671.
<http://dx.doi.org/10.1115/1.1759341>.
16. **Goenka, P.K.; Oh, K.P.** 1986. An optimum short bearing theory for the elastohydrodynamic solution of journal bearings, *ASME Journal of Tribology* 108: 294-299.
<http://dx.doi.org/10.1115/1.3261180>.
17. **Bonneau, D.; Guines, D.; Frêne, J.; Toplosky, J.** 1995. EHD analysis, including structural inertia effects and a mass-conserving cavitation model, *ASME Journal of Tribology* 117: 403-410.
<http://dx.doi.org/10.1115/1.2831288>.
18. **Frêne, J.; Nicolas, D.; Degueurce, B.; Berthe, D.; Godet, M.** 1990. *Lubrification Hydrodynamique. Paliers et Butées-* Eyrolles Editions, Paris.
19. **Booker, J.F.** 1965. Dynamically loaded journal bearings: mobility method of solution, *Journal of Basic Engineering - Transaction of the ASME, series D:* 537-546.
<http://dx.doi.org/10.1115/1.3650602>.

A. Benhamou, A. Bounif, P. Maspeyrot, C. Mansour

JUNGIAMOSIOS TRAUKĖS GUOLIO
ELASTOHIDRODINAMINĖS ANALIZĖS ANALITINIS
TYRIMAS

R e z i u m ė

Elastohidrodinaminiai guolio kakliukai besisukančiose mašinų dalyse veikiami labai sunkių, sukeliančių tepalo sluoksnio plėvelės suplonėjimą, darbo sąlygų gali iššaukti priešlaikinį kontaktinį dilimą. Šiame darbe pasiūly-

tas analitinis minimalaus tepalo plėvelės storio skaičiavimo metodas. Jame įvertintas tampriųjų deformacijų poveikis atsirandantis dėl hidrodinaminio slėgio ir inercijos. Tampriosios deformacijos paskaičiuotos analiniu ir skaitiniu metodu. Jungiamosios traukės-guolio deformacijos buvo įvertintos esant vidutinėms ir mažoms variklio apkrovoms. Analizė atlikta įvertinus inercijos efekto įtaką guolio funkcionavimui stipriai skyrėsi nuo įprastinės. Metodas buvo pritaikytas General Motors variklio jungiamosios traukės-guolio analizei.

A. Benhamou, A. Bounif, P. Maspeyrot, C. Mansour

AN ANALYTICAL APPROACH TOWARDS EHD
ANALYSIS OF CONNECTING-ROD BEARING

S u m m a r y

Elastohydrodynamic (EHD) journal bearings in rotating machine parts are subjected to very severe operat-

ing conditions, leading to a reduction in the minimal thickness of the lubricating film which can generate premature wear of the contact. In this work, an analytical method of calculating the minimal thickness of the oil film was proposed. It takes into account the effect of the elastic deformations due to both hydrodynamic pressure and inertia. The elastic deformations are calculated analytically and simultaneously. The connecting – rod bearing body deformations was predicted under low and moderate engine regimes. The correction produced by the introduction of the effect of inertia, have shown a clear difference for the global behaviour. The method was applied for analysis of a General Motors connecting – rod bearing engine.

Keywords: elastohydrodynamic (EHD), inertia, elastic deformation, oil film thickness.

Received December 13, 2012

Accepted March 05, 2014